Measurements Performed on GaAs - A possible sensor material for the Forward Region of the ILC

Iftach Sadeh

September 2006

Abstract

The next experimental facility for high energy physics agreed upon by the international community of particle physics will be the International Linear Collider. The Forward Region of the Linear Collider will hold several detectors which are expected to absorb amounts of radiation on the scale of 10 MGy/year. In order to produce a viable detector that could withstand these harsh conditions without a degradation of signal, GaAs is considered as the sensor material. Measurements were performed on two samples of GaAs, testing IV (current-voltage) and IT (current-temperature) relations, as well as the CCD's (Charge Collection Distance) dependence on the applied electric field.

This study was done as part of the framework of the DESY Zeuthen 2006 SummerStudent program. I would like to thank the staff in charge of the program, and particularly Wolfgang Lohmann, Ekaterina Kuznetsova, Christian Grah & Alexandr Ignatenko for their frequent support and advice, and for keeping me from destroying too many Keithleys. It's been a great pleasure.

Contents

1 The Very Forward Region of the ILC

The International Linear Collider (ILC) has been agreed upon in a world-wide consensus to be the next large experimental facility in high energy physics. Designs for this machine have been developed in a world-wide effort. The ILC will bring electrons and positrons into collision with an energy of about 500 GeV in the first stage, and 1 TeV in the second stage. The ILC will allow the exploration of the mechanism of electroweak symmetry breaking, and the probing of physics beyond the Standard Model via precision measurements on basic physics processes.

The Forward Region of the ILC will consist of a Beam-Calorimeter, a Luminosity-Calorimeter, and a detector for beamstrahlung photons[1]. The LumiCal is intended to measure small angle Bhabha events: $e^+e^- \rightarrow e^+e^-(\gamma)$, a theoretically well understood process, which can be calculated to very high precision. Effort is made to achieve a theoretical error for this process, which will be better than 10^{-4} [5]. From this follows that one can get an excellent luminosity measurement, with which the cross sections of the important observed processes may be calculated. The BeamCal will be positioned next to the beam pipe covering the lowest possible polar angle, and will also be used for beam-parameters fast tuning (detecting e^+e^- pairs originating from beamstrahlung photon conversion). It will also be very important to have the ability to veto high energy electrons at low polar angles. The electrons may originate from so called two photon processes. The latter are a serious background for supersymmetric processes characterized by missing momentum in the forward region [1]. In addition, the calorimeter shields the inner part of the detector from backscattered beamstrahlung remnants and synchrotron radiation. The PhotoCal or GamCal are detectors designed to measure beamstrahlung photons, which are very collinear to the beam.

[1]Due to the small size and high electric charge of a bunch in the ILC, electromagnetic forces squeeze crossing bunches and cause photon emission. This photon emission is referred to as beamstrahlung.

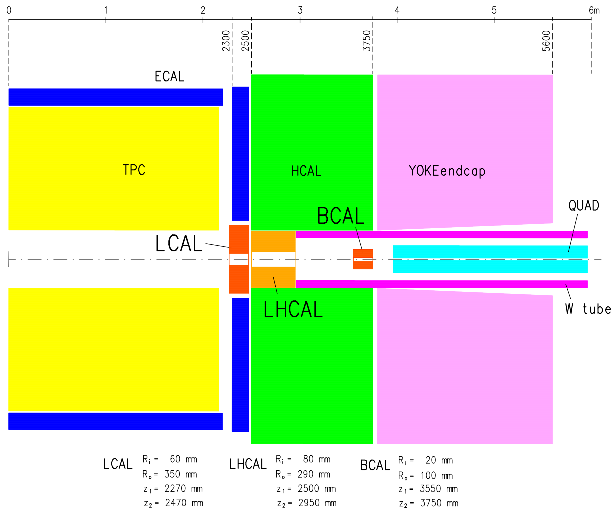

Figure 1: The Very Forward Region of the ILC.

Detector requirements:

- ⋆ To perform the fast beam diagnostics based on the BeamCal measurements, a linear calorimeter response over a large dynamic range is needed.
- ⋆ Measurements of high energy electrons or photons on top of the beamstrahlung background require a small transverse size of the shower developing in the calorimeter.
- ⋆ The beamstrahlung remnants create a huge energy deposition in the BeamCal. The deposited energy depends on the beam parameters and detector design and amounts to about 20 TeV per bunch crossing for the TESLA TDR design [1]. Due to these harsh radiation conditions the active material of the BeamCal must be radiation hard.

Semiconductor materials have proven to be a good solution for these needs.

2 Characteristics of a Semiconductor Detector

A charged particle passing through a semiconductor leaves a track of electron-hole pairs in its wake, which translates to a measurable current. This current is usually scaled in units of Minimum Ionizing Particles (MIPs). A MIP looses a predictable amount of energy while passing through a given thickness of semiconductor material[2]. The charge generated is proportional to the energy deposited in the semiconductor, as it takes a constant value of energy to create an electron-hole pair (ionization energy). This value is a property of the semiconductor, and it depends on its band gap structure. GaAs has a band gap of $E_g \approx 1.42\,\mathrm{eV}$, for which the energy needed to create an electron-hole pair is $E_{(e/h)pair} \approx 4.2\,\mathrm{eV}$ [2].

For an ideal sample of GaAs at 300 °K, the Most Probable Value (MPV) of deposited energy by a MIP is $MIP_{MPV} \approx 0.56\,\frac{\mathrm{keV}}{\mu\mathrm{m}}$. When translating a given measured charge into the energy lost, one must take into account the Charge Collection Efficiency (CCE) of the material, which is defined as the ratio between the charge measured and the charge generated in the material by an ionizing particle. The CCE is a function of the charge carriers' lifetime and drift velocity, which may not necessarily be the same for both electrons and holes. The CCE depends on the interactions inside the material, and consequently on the level of its impurity. The CCE also depends on the strength of the external electric field. The Charge Collection Distance (CCD) is defined as the average distance the charge carriers may travel inside the material before being trapped or recombined. The CCD gives an estimation of the bias voltage needed for operating the detector and also the CCE at a given voltage[3]. Measurements of the CCD of GaAs will be presented in Section 5.3.

[2] The energy loss $\frac{dE}{dx}$ of the charged particle is described by the Bethe-Bloch formula.

[3] This would mean that, for instance, for a sample of 100 μm thickness, a CCD of 75 μm would indicate that the CCE is 75%.

Another characteristic of GaAs is the existence of a leakage current. A small leakage current exists in pure semiconductors due to thermal excitation. This dark current is enhanced by the existence of impurities in the material in the form of extra donors and acceptors. The current's temperature dependence follows [3] :

$$I \backsim exp[-\frac{E_g(T)}{K_B T}], \tag{1}$$

where $E_g(T)$ is the temperature dependant band gap of GaAs. $E_g(T)$ complies with the empirical Varshni relation [6]

$$E_g(T) = E_g^{T=0} - \frac{\alpha\, T^2}{T+\beta}. \tag{2}$$

Here $E_g^{T=0}$ is the band gap at T=0 °K, while α and β are adjustable (Varshni) parameters. For GaAs these values (given here without errors) are

$$E_g^{T=0} \approx 1.517\,\mathrm{eV}, \quad \alpha \approx 5.4 \cdot 10^{-4}\,\tfrac{\mathrm{eV}}{\mathrm{K}}, \quad \beta \approx 204\,\mathrm{K}. \tag{3}$$

The band gap of GaAs will be estimated in Section 5.2.

3 The Effects of Radiation Damage on Semiconductors

The Forward Region of the ILC will be a radiation rich environment, and frequent replacement of the detectors is far from a desirable consequence. This is especially true of the BeamCal, which is expected to absorb up to $10\,\frac{\mathrm{MGy}}{\mathrm{year}}$ [1]. One therefore has to consider the fact that extended radiation exposure may influence the aforementioned properties of a semiconductor. It is general practice to use silicon for manufacturing semiconductor-type detectors. The purpose of this study is to consider an alternative - GaAs, which is believed to be more radiation hard compared to silicon [4].

For semiconductors where the band gap is relatively small, as for silicon, the amount of free charge carriers is high, creating a large amount of noise.

The probability of the recombination of the charge induced by an ionizing particle is increased in this case. Using a reverse biased p-n junction improves the signal to noise ratio. When a semiconductor is exposed to large amounts of radiation, traps are created within it or, alternatively, the effectiveness of traps which are already present is enhanced[4]. The traps absorb the charge induced by the ionizing particle, therefore reducing the CCE. The subsequent change in the internal electric field of the material calls for an increase of the external bias field, in order to keep the depletion zone of the p-n junction wide. Semiconductors with higher band gaps, such as GaAs and diamond, do not need to be doped. They can be used as solid state ionization chambers without the necessity of creating a depletion zone by the use of a bias voltage[5]. In this regard GaAs detectors suffer less from exposure to radiation.

Another point to consider is the effect of radiation on the leakage current. For silicon the leakage current would increase dramatically compared to that of GaAs. A drawback of GaAs compared to silicon, is that extended radiation damage causes less degradation of the signal of a MIP for silicon, than for GaAs. One must then balance the advantages and disadvantages of either material.

Other sensor material options are also being considered, particularly that of a CVD diamond detector. This complimentary study is discussed in [1].

4 The Experimental Setup

In order to be able to interpret the readings of a GaAs calorimeter, several factors need to be taken into account, namely, the IV (current-voltage) and

[4]The existence of traps beforehand is, practically speaking, unavoidable, due to impurities and structure imperfections.

[5]A bias voltage is needed for GaAs detectors in order to prevent the charge carriers from recombining. Applying it also increases the charge carriers' mobility, and subsequently improves the CCE. These factors, though, do not demand a massive increase in the bias voltage due to radiation damage.

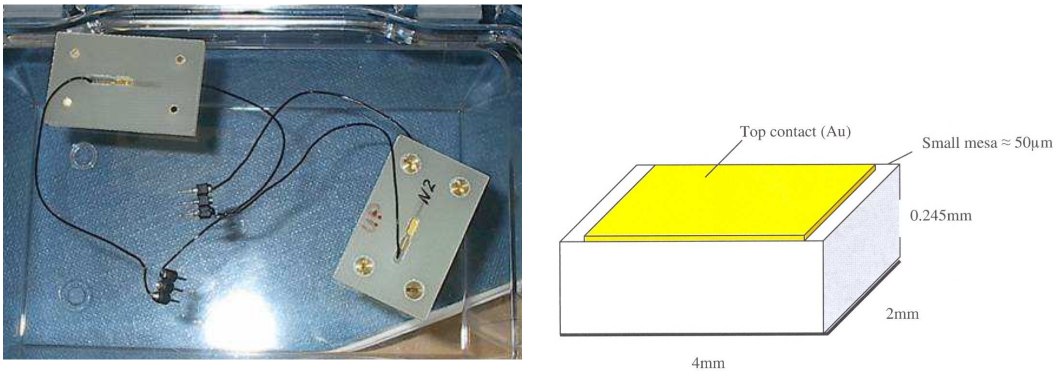

Figure 2: Two samples of GaAs, denoted as GaAs2 & GaAs3
Left: A picture of the samples which are mounted on frames. Right: Schematic description of a sample.

IT (current-temperature) characteristics of the detector, and it's CCD.

Two GaAs samples were used. The samples were produced in JINR, Dubna. Their dimensions were $4 \times 2 \times 0.245\ \mathrm{mm}^3$, with metal (Au) contacts on both sides, as shown in Figure 2. They will be referred to as GaAs2 and GaAs3 [6].

4.1 IV Measurements

Current-voltage measurements were performed for the GaAs samples. A sample was placed inside a "black-box" for light and electrical shielding, and the current was measured for different settings of the bias voltage. The voltage was supplied and the current was measured by means of a Keithley 487 Picoammeter. The voltage was ramped up in the range [0,250]V in 25V intervals, and then down all the way back. Each voltage value was applied for 300 seconds and the results from the last 20% of the measurements were

[6] The terminology of "forward" and "reverse" bias will henceforth be used in regard to the samples. This is just a convention chosen by the manufacturer in order to distinguishes between the "top" and "bottom" sides of the sample, and has no deeper meaning.

averaged[7]. The measurements were repeated for both the forward and the reverse bias settings. Several sets of these measurements were taken for both of the samples. The temperature inside the black-box was recorded once per measurement using a simple thermometer.

4.2 IT Measurements

Current-temperature measurements were also performed on both samples. A sample was placed on a fiberglass support which was installed inside a small metal box. The box was encapsulated by a layer of Styrofoam in order to thermally insulate its content. Two temperature sensors were placed near the sample in two configurations. In the first, both sensors were placed very close to the sample thus measuring the temperature of the surrounding air. In the second configuration one sensor was in the air while the other touched the fiberglass support. Finally, the setup was placed on top of a heating plate. The bias voltage was supplied by a Keithley 487 Picoammeter. The temperature and the current were measured by a Keithley 2700 Data Acquisition System.

Measurements of the temperature and of the current through the sample were taken for a fixed value of the bias voltage. This was done while the heating plate was activated, and after it was deactivated. While the plate was activated, it turned itself on and off repeatedly sending bursts of heat into the system. When the temperature which was measured inside the box reached $\sim 350\,^{\circ}K$ the heating plate was deactivated, and the system cooled down to room temperature without intervention. These measurements were performed on both samples in the various configurations, for bias voltages of 25V, 50V and 75V.

[7]The initial range of values was discounted in order to let the sample stabilize under a given voltage.

4.3 CCD Measurements

Charge Collection Distance measurements were performed on GaAs2. A schematic representation of the setup is shown in Figure 3. A ^{90}Sr β source was placed over a metalized box with the sample and the preamplifier (PA). The electron beam was defined by (one 5 mm aperture and one 2 mm aperture) brass collimators adjacent to the source. A lead collimator below the sample prevented electrons, that might not have traveled through the GaAs itself, from hitting the scintillator[8]. Two photomultiplier tubes (PMTs) received the signal from the scintillator. The threshold setting of the discriminators (DISCR) determined whether a signal was detected by the corresponding PMT. A gate was applied to the signal, which was passed on only in the case of a coincidence by the use of an AND gate and a timer. The ADC sent the result of the signal charge measurement to a PC. The bias voltage was provided, and the current and temperature were measured by a Keithley 6487 Picoammeter. The temperature was measured in the vicinity of the sample. The devices were controlled by a LabView program. Pedestal (noise) measurements were performed before each measurement by the use of a pulse generator applying a random trigger signal to the ADC. The current was monitored continuously. Measurements on the GaAs2 sample were performed in the bias voltage range of [5,450]V, corresponding to [0.02,1.84]$\frac{\mathrm{V}}{\mu\mathrm{m}}$.

[8] The β radiation source emits electrons with varying amounts of energy. The purpose of the experiment was to measure the signal of MIPs. Therefore, only electrons which were energetic enough to traverse the entire depth of the sample, and actually did so, were taken into account.

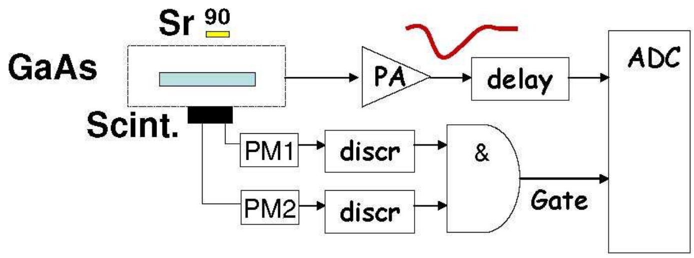

Figure 3: The CCD Measurement Setup.

5 Results

5.1 IV Measurements

In Figure 4 the results for the current-voltage measurements of GaAs2 are shown. Similar results were obtained for GaAs3. The existence of a dark current was mentioned in Section 2. Comparing the forward and reversed bias tests, one can see that a hysteresis occurs. This non-linear behavior is expected due to the change of the internal electrical field of the material as a result of the exposure to the strong external bias field.

Another important observation is that the IV characteristics of GaAs are strongly temperature dependant.

5.2 IT Measurements

Since it is impossible to directly touch a GaAs sample during an experiment, as this would pollute it, estimating an exact temperature reading of the sample to a high precision was difficult. Two approaches were taken to resolve this problem.

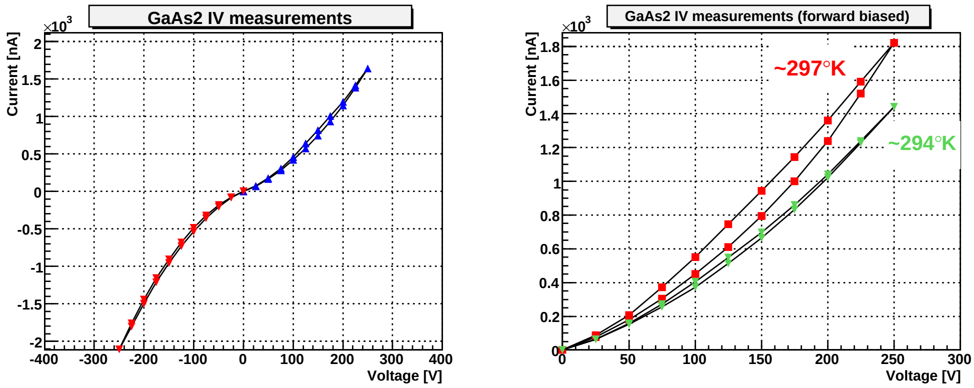

Figure 4: GaAs2 IV Measurements.

Left: Forward and reversed bias voltage measurements. Right: Two forward biased measurements done consecutively at slightly different temperatures (temperature values are an approximation).

5.2.1 Measurements Done With the GaAs2 Sample

Representations of the temperature-time and of the current-temperature profiles are shown in Figure 5.

Both temperature sensors were placed in the air near the GaAs2 sample. The readings from the two sensors were averaged, and this average was later used as the temperature measurement for a given point in time. The values from the two channels coincided with an accuracy of 0.6 °K. A notable difference is seen between the heating and the cooling periods. One would expect to observe a single backtracking line, as no difference should be apparent in the sample for a given temperature and fixed voltage. This difference represents the systematic error in the experiment. In order to converge the values of current per temperature, the measurements were binned into discret temperature values of 1 °K width, and averaging was performed on both the temperature and the current within these bins. The averaged sets for each of the three bias voltage settings are presented in Figure 6. The error bars are due to the averaging procedure and stand for the aforementioned systematic

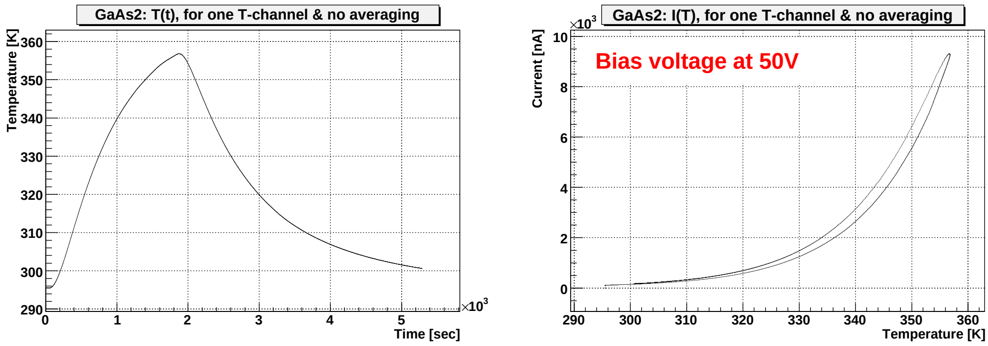

Figure 5: GaAs2 IT Measurements.

Left: Temperature vs. time profile. Right: Current vs. temperature profile.

error. Fitting was done with

$$Log[I] \backsim -\frac{E_g(T)}{K_B T} \to p_0 + \frac{p_1}{T} \tag{4}$$

for the parameters p_0 and p_1. This is just the logarithm of Equation 1, as it proved to be more stable for the purpose of the numerical calculations. The lines in Figure 6 are the result of the fittings. The values for the fitting parameters are given in Table 1.

5.2.2 Measurements Done With the GaAs3 Sample

For measurements done with the GaAs3 sample, the position of one of the temperature sensors was shifted to the support on which the sample was mounted, while the other sensor remained in the air. This change resulted in a notable difference between the two temperature channels, and so only readings from the sensor touching the fiberglass support were taken into account. The resulting current-time profile showed a difference of no more than 0.2 nA between the heating and the cooling periods. This difference is generally smaller compared to the one achieved for GaAs2 in Section 5.2.1. The results are shown in Figure 7.

Because of the large systematic errors of the measurements done with the

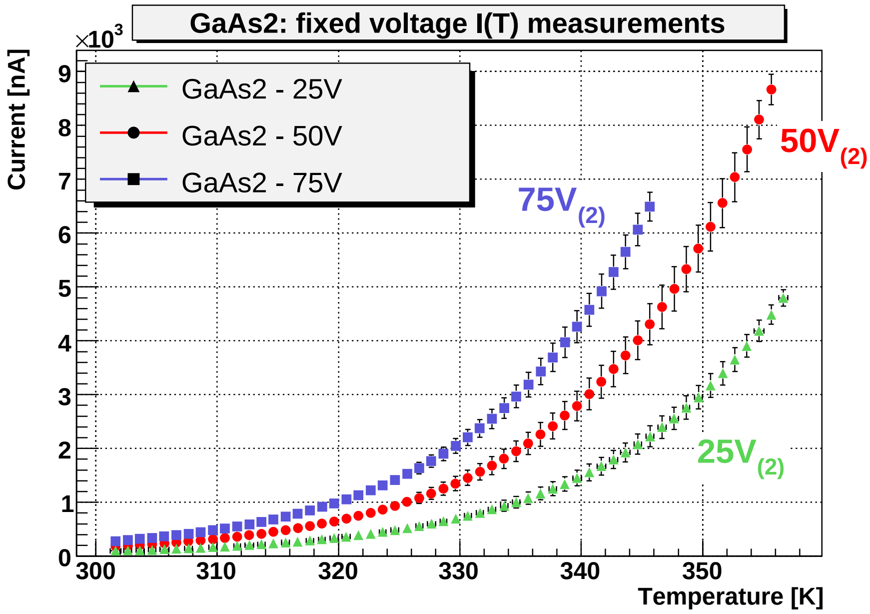

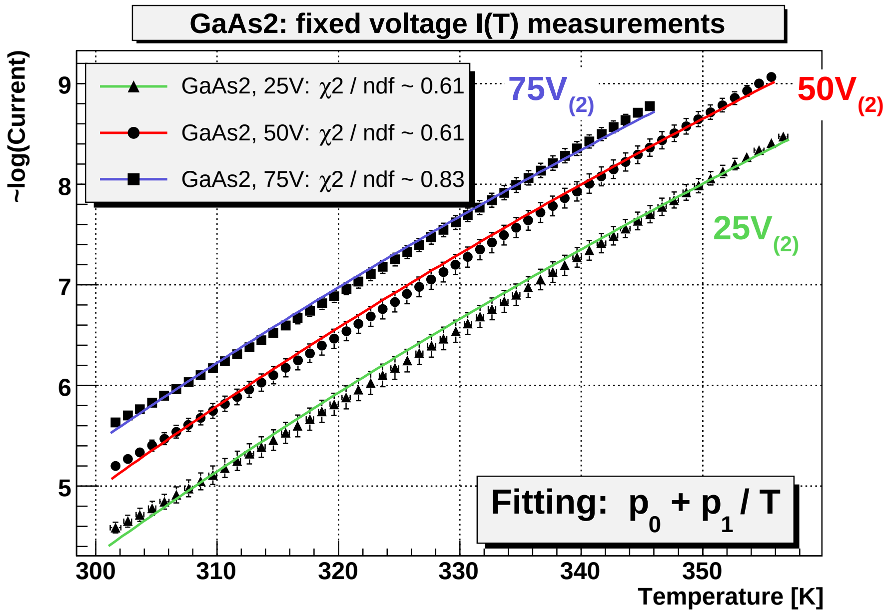

Figure 6: GaAs2 IT Measurements.

Top: Current vs. temperature measurements for $25V$, $50V$ and $75V$ bias voltage settings (averaged over sensor channels & temperature bins). Bottom: A fitting for the results, done in logarithmic scale.

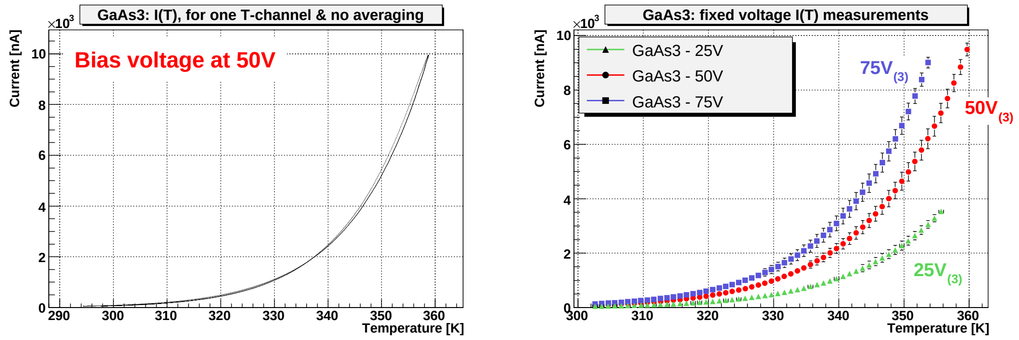

Figure 7: GaAs3 IT Measurements.

Left: Current vs. temperature profile for the sensor that was placed on the support upon which the sample was resting (the reader may compare with the plot on the right side of Figure 5). Right: Current vs. temperature measurements for $25V$, $50V$ and $75V$ bias voltage settings (for one temperature channel, and for the heating period only).

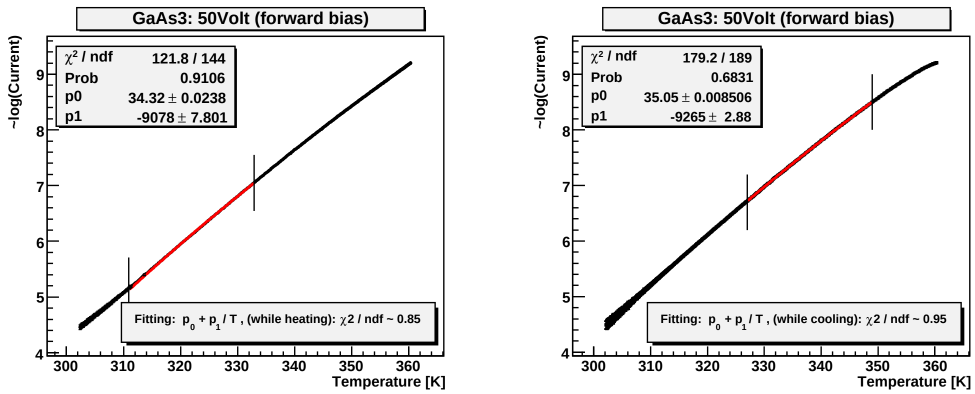

Figure 8: GaAs3 IT Measurements - Fitting done in logarithmic scale.

The vertical lines mark the range in which the fitting was performed. The line thickness in the low range of temperature is due to large error bars. Left: Fitting done in the $[311, 333]\,°$K temperature range in the heating phase. Right: Fitting done in the $[327, 249]\,°$K temperature range in the cooling phase.

GaAs2 sample, for GaAs3 a different analysis approach was implemented. In this case no averaging of the temperature or current into bins was made. Instead, separate fits were performed for the heating and for the cooling periods. Also, so as to improve the quality of the fit, each period was divided into two segments, and fitting was done separately. All in all, for three bias voltages, two temperature ranges, and two thermal gradients (heating and cooling), 12 separate fits were performed. The results are presented in Table 1. A typical graphical example is given in Figure 8.

5.2.3 Comparison Between the Two Sets of Results and Estimation of the Fitting Parameters

A visual comparison between the measurements of the two samples is shown in Figure 9. It is clear that the two samples are different, regardless of the difference in temperature measuring techniques[9]. While the same behavior with regard to the change of temperature or bias voltage seems apparent in both samples, the differences between the two are worth noting. These differences must be resolved to a coherent standard of behavior, if GaAs is to be considered for detector use.

From Equations 2 and 3, the GaAs band gap can be determined. In the range of temperature, in which the experiment was performed - $[310, 350]\,^\circ$K, we get $E_g^{GaAs} \sim 1.41 \pm 0.02$ eV. Using Equation 4 one may compare this value with the fitting parameter p_1. The comparison is presented in Table 1. An average of the different results shown above was taken for GaAs2, assuming for simplicity that the errors are not correlated. For GaAs3 no averaging was performed since the different fitting results differ too much, and are not within a few standard deviations of each other. Instead, the highest and lowest values of the fitting parameter p_1 were used to compute lower and upper bounds on the band gap energy.

[9]The temperature difference between the two sensor channels during the GaAs3 measurements was of the order of $\sim 2\,^\circ$K at most and can't account for this.

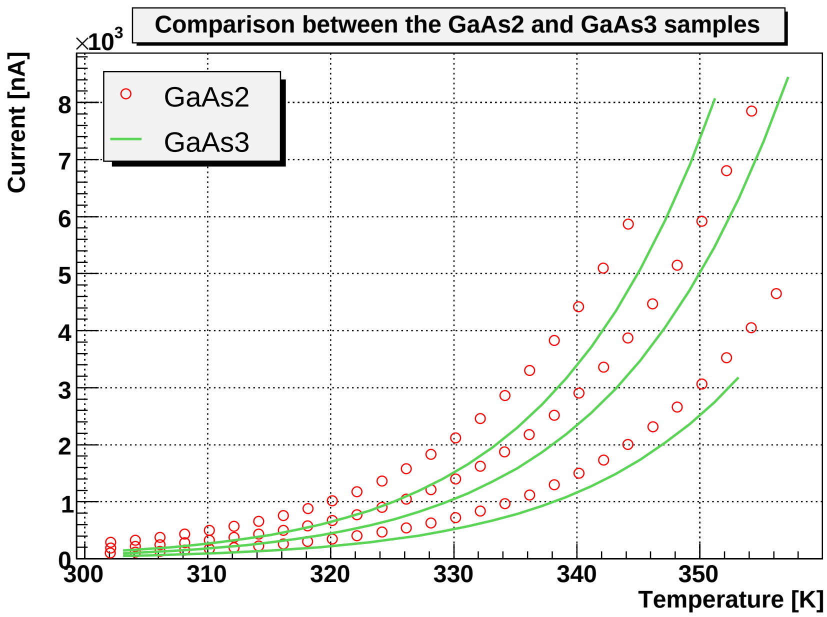

Figure 9: Comparison between GaAs2 & GaAs3

Current vs. temperature measurements for $25V$ (lowest), $50V$ (middle) and $75V$ (highest) bias voltage settings. GaAs2 is marked with circles and GaAs3 with lines.

Table 1: RESULTS FOR THE FITTING ACCORDING TO: $(p_0 + \frac{p_1}{T})$
THE READER MAY COMPARE WITH THE BAND GAP OF GaAs:
$\underline{E_g^{GaAs} \sim 1.41 \pm 0.02 \text{ eV}}$

THE FITTING PARAMETER $(-p_1)$ FOR THE GaAs2 SAMPLE
(FOR DIFFERENT BIAS VOLTAGES)

$25V$	$50V$	$75V$
7747 ± 62	7743 ± 57	7742 ± 59

$\rightarrow$ AVERAGED: $\underline{7743 \pm 34 \text{ K}^{-1}}$

GaAs2 band gap from the averaging of (p_1) : $\underline{E_g^{F2} = 0.667 \pm 0.005 \text{ eV}}$
(The errors are considered to be uncorrelated)

THE FITTING PARAMETER $(-p_1)$ FOR THE GaAs3 SAMPLE
(FOR DIFFERENT BIAS VOLTAGES & TEMPERATURE RANGES/GRADIENTS)

	$[311, 333]\,^\circ$K		$[327, 349]\,^\circ$K	
	HEATING	COOLING	HEATING	COOLING
$25V$	9442 ± 19	9085 ± 12	9602 ± 5	9152 ± 4
$50V$	9078 ± 8	9140 ± 6	9371 ± 3	9265 ± 43
$75V$	9443 ± 5	9053 ± 4	9545 ± 2	9091 ± 3

Lower and upper bounds on the GaAs3 band gap from the values of p_1 :
$\underline{E_g^{F3-low} = 0.780 \pm 0.001 \text{ eV}} \longleftrightarrow \underline{E_g^{F3-up} = 0.823 \pm 0.001 \text{ eV}}$

5.3 CCD Measurements

A typical histogram of a signal of a MIP is shown in Figure 10. The noise peak is clearly separated from the MIP signal peak, and therefore each may be fitted individually. As the bias voltage was increased, distinguishing between the two peaks became less easy, but up to the maximum voltage which was used here, $450\text{V} \leftrightarrow 1.84\,\frac{\text{V}}{\mu\text{m}}$, it was always possible. The pedestal in Figure 10 is a Gaussian, while the MIP is a Landau distribution convoluted with a Gaussian[10]. The CCD was calculated according to

$$CCD \equiv (L_{MPV} - G_{Mean}) \cdot \frac{ADC_{e/channel}}{MIP_{MPV}/E_{(e/h)pair}} \tag{5}$$

where the ADC channel is converted to the number of electron-hole pairs produced, and this translated into energy using the MPV of a MIP according to the Landau distribution L_{MPV} (discounting the pedestal, G_{MPV}), and the energy to create an electron-hole pair in GaAs, $E_{(e/h)pair}$ (see Section 2).

MIP signals were measured for various voltage settings, and the CCD was calculated accordingly. The results are shown in Figure 11, where the CCD is plotted against the voltage per unit thickness (in μm) of the GaAs sample.

[10]The reason for this is the fluctuation in the charge velocity inside the material, from the point of the creation of the electron-hole pair by the MIP, to the electrodes where the leakage current is collected .

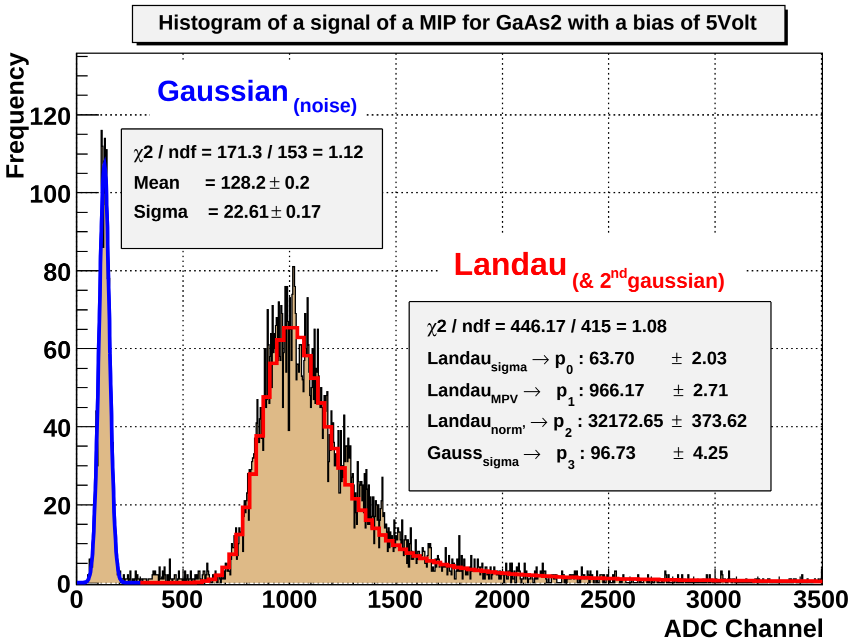

Figure 10: Typical histogram of a signal of a MIP for GaAs2 Two signals can be seen. On the left the sharp peek is the pedestal (noise) and on the right the signal of the MIP. The two can easily be separated and fitted individually, as was done here. The MIP is fitted according to a Landau distribution convoluted with a Gaussian.

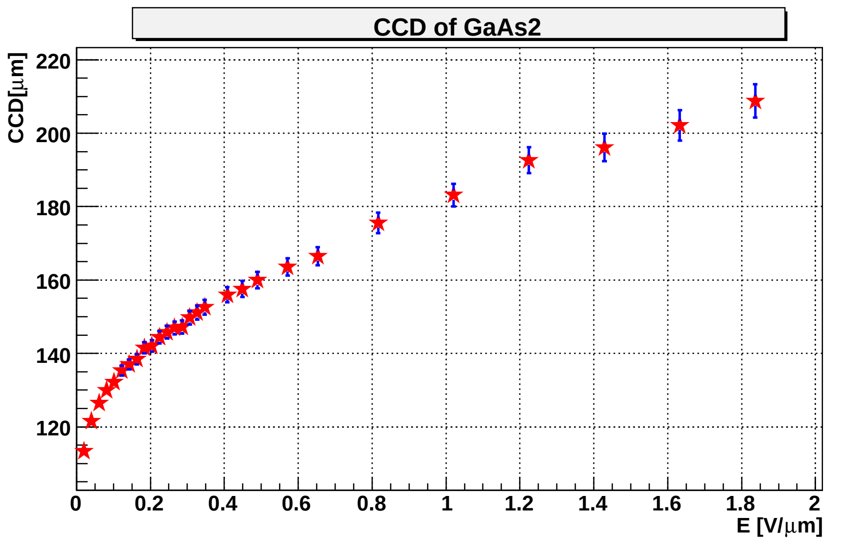

Figure 11: CCD vs. voltage-per-unit-thickness for GaAs2

6 Summary and Discussion

The next large experimental facility in high energy physics is going to be the ILC, and the time is approaching when the design of the detectors of the forward region will have to be finalized. The purpose of this study has been to explore some of the properties of GaAs, which must be known, if GaAs is to be considered as the sensor material for these detectors.

In Section 5.1 the IV characteristics of GaAs were tested. It was shown that a hysteresis occurs, and that the current-voltage relationship is strongly temperature dependant. In Section 5.2 this relationship was explored in depth. Two different measurement schemes were used in order to determine the IT dependence of the GaAs samples. An effort was made to overcome the difficulty of measuring the real-time temperature of a sample, while not being able to put it in thermal equilibrium with a temperature sensor. The fitting results of these measurements were then held up against the theoretically predicted value of the energy band gap of GaAs in the relevant temperature range $E_g^{GaAs} \sim 1.41 \pm 0.02$ eV. In Section 5.3 the CCD of GaAs was tested. Measurements were made in the bias voltage range of [5,450]V, corresponding to $[0.02,1.84]\frac{\mathrm{V}}{\mu\mathrm{m}}$.

Table 1 summarizes the fitting results of the IT measurements for the two samples. For GaAs2 we have the averaged band gap value $E_g^{F2} = 0.667 \pm 0.005$ eV, while for GaAs3 we have lower and upper bounds on the band gap $E_g^{F3-low} = 0.780 \pm 0.001$ eV and $E_g^{F3-up} = 0.823 \pm 0.001$ eV. When comparing these results to the theoretical value one should take into account several factors. First, the theoretical model used here is only a first order approximation. The energy band structure of GaAs is more complicated than that which was discussed above. Intermediate local states exist in the band gap due to impurities and to imperfections within the crystal. These states contribute to the likelihood of charge carriers moving into the conduction band. The contribution is, naturally, temperature dependant. The existence of traps due to radiation damage also changes this probability. These factors tend to reduce the effective band gap and therefore improve the results obtained here. Another point to consider is the existence of the metal plates on either end of the samples. The metal contact contributes to a changed Fermi level near the boundaries (in fact, a small Schottky diode effect). The significance of this change depends on the temperature as well.

Systematic errors must also be taken into account. The range of temperature in which the measurements were taken is limited, and the uncertainties in measuring the actual real-time temperature of the samples are discussed above. In order to improve the results presented here, one should perform the measurements in a controllable and stable range of temperature, in which the GaAs could reach thermal equilibrium with its environment. A heat bath would then have to be introduced into the system, for instance, in the form of a copper plate. This plate would replace the fiberglass support of the sample. The good thermal conductance of the plate would allow for the sample to be heated efficiently, and its high thermal capacitance would make it possible to attach a temperature sensor directly to it. The sensor would then measure the temperature of the bath, which would be in equilibrium with the temperature of the GaAs sample.

Figure 11 shows the CCD measurements which were performed. Its obvious that the CCD changes more rapidly for different bias voltages in the low voltage range $[0.02,0.65]\frac{\mathrm{V}}{\mu\mathrm{m}}$ than for higher values. This is crucial information, since it is desirable for a sensor to operate with a bias voltage that imposes a known and stable value of CCD, which is equivalent to knowing the CCE. The CCE determines the error with which the charge that is measured is translated into the energy that was deposited in the sensor.

The purpose of the next phase of experiments will be to determine the nature of the damage done to GaAs due to exposure to large amounts of radiation. The predicted change of the IV characteristics and the CCD's dependence on bias voltage [4] will then be checked.

References

[1] H. Abramowicz, *et al.*, R&D for the ILC-Detector: Instumentation of the Very Forward Region (2006), http://www-zeuthen.desy.de/ILC/fcal

[2] R. Bates, *et al.*, Radiation Induced Damage in GaAs Particle Detectors (1997), arXiv.org:physics/9709034

[3] H. G. Svavarsson, *et al.*, Impurity band in lithium-diffused and annealed GaAs: Conductivity and Hall effect measurements, PHYSICAL REVIEW B 67, 205213 (2003)

[4] Jörg Breibach, Development of GaAs Pixel Detectors (2000), PITHA 00/14

[5] H. Abramowicz, R. Ingbir, S. Kananov, and A. Levy. Monte Carlo study of a luminosity detector for the International Linear Collider. arXiv.org:physics/0508074, 2005.

[6] I. Vurgaftman & J. R. Meyer, Band parameters for III-V compound semiconductors and their alloys, journal of applied physics - vol' 89, number 11 (2001)